

PACS numbers: 42.25.Dd; 42.62.Be; 02.50.Ng
DOI: 10.1070/QE2002v032n10ABEH002310

Monte Carlo simulation of laser beam propagation in a plane layer of the erythrocyte suspension: comparison of contributions from different scattering orders to the angular distribution of light intensity

M.Yu. Kirillin, A.V. Priezzhev

Abstract. **The scattering phase functions of light are obtained for a layer of the erythrocyte suspension by the Monte Carlo method. At the erythrocyte concentration corresponding to the whole blood, these functions substantially differ from the phase function of a single erythrocyte. Contributions from the low-order and multiple scattering to the light intensity measured at different angles are compared. It is shown that scattering of light from a suspension layer of thickness of about 100 μm to the forward half-plane is mainly determined by the low-order scattering (by snake photons), whereas scattering to the back half-plane is mainly determined by multiple scattering. The possibility of using the diffuse approximation for the theoretical description of scattering is analysed.**

Keywords: *propagation of light in a scattering medium, scattering indicatrix, scattering anisotropy factor, laser medicine.*

1. Introduction

The development of new methods for laser medical diagnostics [1] requires detailed studies of light propagation in tissues, in particular, blood. This process substantially depends on the absorption and scattering coefficients, the anisotropy factor, and the scattering function of a tissue [2]. Theoretical approaches for solving this problem for a suspension of particles were developed in a number of papers (see, for example, [3 – 5]). However, in most cases, the assumptions, which were used in the development of these methods, did not take into account adequately the properties of the whole blood as a dense erythrocyte suspension. The experimental studies of the propagation of a laser beam through a blood layer are complicated by the problem of maintaining constant structural and dynamic parameters of the whole blood. For this reason, the role of computer simulations, in particular, Monte Carlo simulations [6] becomes increasingly important. The Monte Carlo method is based on the repeated calculations of a photon trajectory in a scattering and absorbing medium followed by the generalisation and statistical averaging of the data obtained.

Because the optical properties of the whole blood are close to those of an erythrocyte suspension, experiments are often performed with suspensions of washed out erythrocytes in a buffer solution with the volume concentration (hematocrit Hct) equal to that in the whole blood (Hct $\approx$ 40 %). In such a suspension, constant structural and dynamic parameters and, hence, optical parameters can be maintained more easily, and in particular, the aggregation of red blood cells can be avoided.

The aim of this paper is to simulate the propagation of laser radiation in a layer of a suspension of non-aggregated erythrocytes, to compare the contributions from different scattering orders to the angular distribution of scattered light and to elucidate the possibility of application of the diffuse approximation for solving this problem.

The main problem in the simulation of biological objects is to choose an adequate model, which would reflect the basic properties of a real object. Erythrocytes are cells without nuclei, which have the form of a biconcave disc of diameter 7.1 – 9.2 μm and a maximum thickness of 1.7 – 2.4 μm [7]. The erythrocyte volume is 70 – 100 μm^3. During various pathologies, normal erythrocytes (discocytes) can change their form without volume changing. Erythrocytes consist of a very thin membrane (of thickness $\sim$ 25 nm) and an almost saturated hemoglobin solution. An erythrocyte contains about 70 % of water, 25 % of hemoglobin, and 5 % of lipids, sugars, salts, enzymes, and proteins. Optically, erythrocytes belong to soft particles: the real part of their refractive index weakly differs from the refractive index of the environmental plasma. For example, the relative refractive index at a wavelength of 0.66 μm is $n_{rel} = 1.037$ [8] and at 0.514 μm, $n_{rel} = 1.040$ [9].

Because the phase scattering function of a single erythrocyte depends on its orientation [10], different approximations are used in calculations. All these approximations take into account that the angular distribution of light scattered from many randomly distributed nonspherical particles is the same as that for scattering from randomly distributed spheres of the same volume. In our model, erythrocytes are represented by spheres, which are characterised by the phase scattering function and the anisotropy factor g of the medium. This factor is a mean cosine of the scattering angle for a single erythrocyte ($g = 0.950 - 0.999$).

M.Yu. Kirillin, A.V. Priezzhev International Teaching and Research Laser Center, M.V. Lomonosov Moscow State University, Vorob'evy gory, 119992 Moscow, Russia

Received 28 February 2002
Kvantovaya Elektronika **32** (10) 883 – 887 (2002)
Translated by M.N. Sapozhnikov

2. Simulated experiment and basic model relations

The parameters of our model correspond to the conditions of the experiment performed with the help of a goniophotometer described in paper [11]. The authors of this paper measured the scattering phase function for an erythrocyte suspension of healthy donors. Erythrocytes were separated from plasma and other blood components by centrifuging. The washed off erythrocytes were used to prepare a suspension with the hematocrit Hct = 40 % corresponding to the whole blood. Experiments were performed with completely oxygenised erythrocytes. A plane-parallel glass cell of thickness 100 μm was filled with the suspension and placed to water to compensate for light refraction at the interface between two media. A cw argon laser emitting at 0.514 μm was used as a source of probe radiation. A collimated laser beam was incident normally to the cell surface. Radiation scattered by blood at angles from zero to 180° was detected with a photodetector, which could be moved by steps along a circle in the scattering plane. The scattering indicatrix of a blood layer being probed was plotted using the photodetector signals.

We simulated the suspension as a suspension of spherical particles with the scattering coefficient μ_s, absorption coefficient μ_a, the anisotropy factor g, and the scattering phase function $P(\boldsymbol{s}, \boldsymbol{s}')$ of a single erythrocyte (where $\boldsymbol{s}$ and $\boldsymbol{s}'$ are the unit vectors of the photon velocity before and after scattering). We used the values of parameters μ_s, μ_a and g calculated from experimental data obtained for the whole non-aggregated blood [11, 12] (Table 1).

Table 1. Optical parameters of the whole blood (Hct = 40 %) for two wavelengths.

Wavelength/μm	μ_s/mm^{-1}	μ_a/mm^{-1}	g	References
0.514	221	22.7	0.972	[11]
0.633	85	0.6	0.980	[12]

The mean free path L is determined by the probability density function. According to [13], we represent this function in the form

$$P(L) = \frac{1}{\langle L \rangle} \exp\left(-\frac{L}{\langle L \rangle}\right),$$

where the mean free path is

$$\langle L \rangle = \frac{1}{\mu_s + \mu_a}.$$

Because

$$\int_0^\infty P(L)\mathrm{d}L = 1,$$

the mean free path is calculated by using a random number,

$$\xi = \int_0^L P(l)\mathrm{d}l,$$

which is uniformly distributed in the interval (0, 1) and is generated by a random-number generator. Thus, we have

$$L = -\frac{\ln(1-\xi)}{\langle L \rangle}.$$

The scattering angle is determined by the scattering phase function

$$P(\boldsymbol{s}, \boldsymbol{s}') = P(\theta)P(\varphi),$$

where θ and φ are the spherical coordinates of the velocity vector of a scattered photon in the reference system related to a scatterer. We assume that scattering particles (erythrocytes) are spherically symmetric. Such an approximation is often used in similar cases and it is based on the fact that a photon propagating through a suspension of particles collides with the particles at different angles. Therefore, we can use an averaged scattering indicatrix. The use of this model in other papers [14, 15] and a comparison of numerical calculations with experimental results [12, 15] showed that this approximation adequately describes the properties of most biological tissues, including blood.

In this approximation, we have $P(\varphi) = 1/(2\pi)$ due to the symmetry. For particles of size substantially exceeding the light wavelength, the scattering indicatrix is strongly elongated forward. It was shown in a number of papers [12, 14, 15] that $P(\theta)$ can be approximated with good accuracy by the empirical Henney–Greenstein function

$$P(\theta) = \frac{1}{4\pi} \frac{1-g^2}{(1+g^2-2g\cos\theta)^{3/2}}.$$

It is this approximation that we used in our calculations.

We simulated the propagation of light in blood at two wavelengths 0.514 and 0.633 μm, which are most often used in experiments. The wavelength 0.514 μm coincides with the maximum of the absorption spectrum of the blood determined by hemoglobin, while the wavelength 0.633 μm lies within the so-called transparency window (0.6–1.5 μm). The light wavelength is specified implicitly by the parameters μ_s, μ_a, g determined experimentally (Table 1). A sample being simulated is a plane layer of the erythrocyte suspension of thickness $d = 0.1$ mm, which has the refractive index $n = 1.35$ corresponding to a suspending liquid.

The model takes into account optical effects taking place at the cell-medium interface. Each calculation was performed for 5×10^5 photons. To shorten the calculation time, we simulated absorption of photons by reducing their initial conditional parameter, the so-called weight, which was assumed equal to 20 here (the weight was taken as a number that was close to the value $\mu_s d$). After each statistical absorption event, the weight decreased by unity. The propagation of a photon is interrupted and monitoring of the photon trajectory is terminated only when the weight vanishes. We simulated a laser beam by an infinitely narrow beam because our preliminary calculations showed that scattering indicatrices obtained for Gaussian beams of different diameters coincide, within the error, with the results obtained for an infinitely narrow beam. This is explained by the fact that the angular characteristics of a photon, propagating in a plane layer with randomly distributed scatterers, are independent of the point of its entrance into the medium. A simulated photodetector had the angular resolution 0.005 rad. To enhance the statistical validity of the results, we performed integration over the

entire sphere, where light was scattered, because the simulated experiment was axially symmetric with respect to the laser beam.

3. Results and discussion

We simulated complete scattering phase functions and the contributions to the phase function made by photons involved in different numbers of scattering events (Figs 1 and 2). In addition, we obtained for both wavelengths the dependences of the contribution to the total signal (scattered light intensity) on the scattering order (Figs 3 and 4).

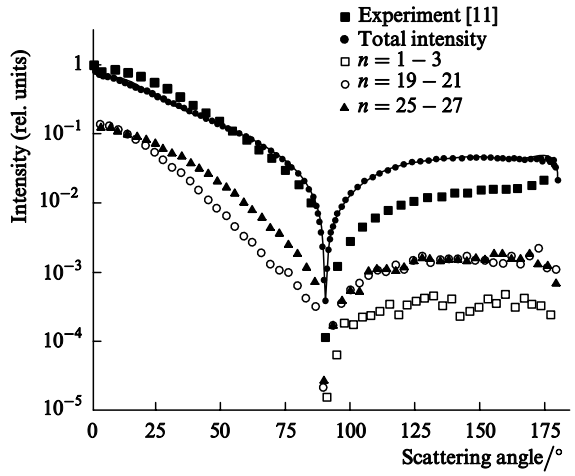

Figure 1. Scattering indicatrices corresponding to total scattering and scattering of different orders n for $\lambda = 0.514$ μm, $\mu_s = 211$ mm^{-1}, $\mu_a = 22.7$ mm^{-1}, $g = 0.972$, $d = 0.1$ mm. The calculation was performed for 5×10^7 photons.

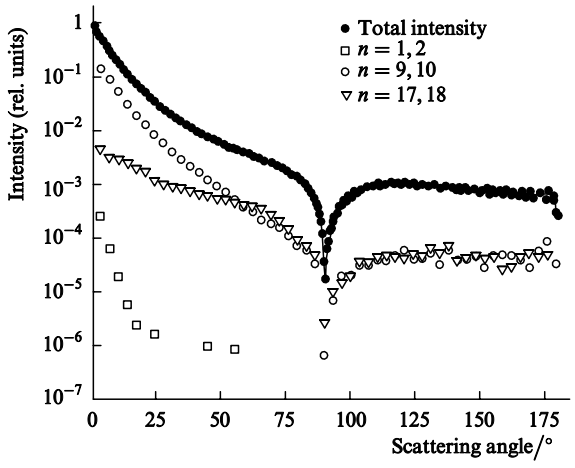

Figure 2. Scattering indicatrices corresponding to total scattering and scattering of different orders n for $\lambda = 0.633$ μm, $\mu_s = 85$ mm^{-1}, $\mu_a = 0.6$ mm^{-1}, $g = 0.980$, $d = 0.1$ mm. The calculation was performed for 5×10^7 photons.

One can see from Figs 3 and 4 that scattering to the forward half-plane in both cases is determined by low-order scattering, with the order close to $d\mu_s$. This is explained by the fact that the scattering indicatrix of a single erythrocyte is strongly elongated forward, and when a photon experiences only a small number of scattering events during its propagation to a detector, the deviation of the maximum number of photons from the initial direction will be small. Such photons are called snake photons. The thickness of a layer of the erythrocyte suspension in our model was only 0.1 mm. The plots presented in Figs 3 and 4 show that most of the 0.514-μm photons ($\mu_s = 221$ mm^{-1}) experience about 22 scattering events, while the 0.633-μm photons ($\mu_s = 85$ mm^{-1}) experience about 10 scattering events. Therefore, the signal is mainly determined by snake photons that have undergone multiple scattering in the medium without a substantial change in the propagation direction.

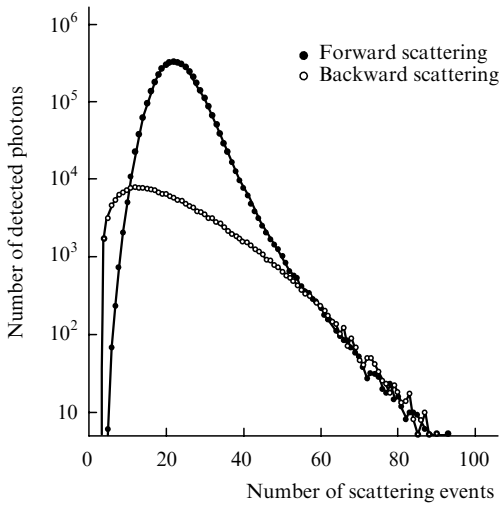

Figure 3. Dependences of the number of detected photons on the number of scattering events experienced by them for $\lambda = 0.514$ μm, $\mu_s = 221$ mm^{-1}, $\mu_a = 22.7$ mm^{-1}, $g = 0.972$, $d = 0.1$ mm. The calculation was performed for 5×10^7 photons.

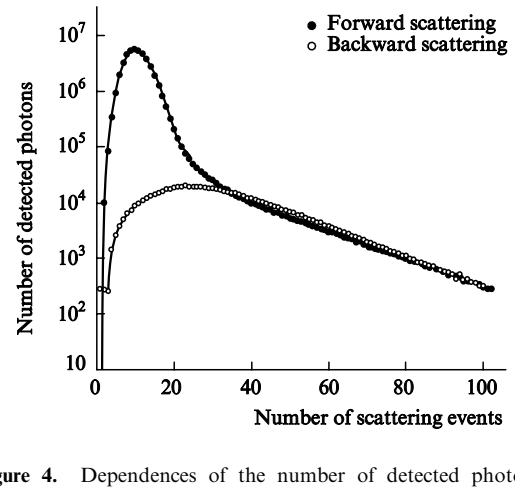

Figure 4. Dependences of the number of detected photons on the number of scattering events experienced by them for $\lambda = 0.633$ μm, $\mu_s = 85$ mm^{-1}, $\mu_a = 0.6$ mm^{-1}, $g = 0.980$, $d = 0.1$ mm. The calculation was performed for 5×10^7 photons.

Analysis of the dependences of the scattering function on the number of scattering events experienced by photons (Figs 1 and 2) also shows that snake photons make the main contribution to scattering to the forward half-plane. This is demonstrated by a drastic decrease in the intensity of detected radiation with increasing scattering angle. For

$\lambda = 0.633$ μm, the low-order scattering functions fall stronger at small scattering angles than the total scattering function (Fig. 2), which means that most photons deviate from the initial direction even weaker than for $\lambda = 0.514$ nm. This is explained by the fact that the parameter μ_s for $\lambda = 0.633$ μm is lower than for $\lambda = 0.514$ μm and, hence, each photon will experience on average less scattering events, and the deviation from the initial propagation direction will be also smaller.

It is important to detect light scattering to the back halfplane in the studies of blood. This is explained by the fact that in many *in vitro* experiments with blood samples and especially in experiments *in vivo*, a backward scattering signal is usually detected because a detector is placed from the same side as a source. One can see from the diagrams of backward scattering that low-order scattering virtually does not contribute to this signal, which is again caused by a strong forward elongation of the scattering diagram for a single erythrocyte. One can also see that the dependence of the contribution of photons on the scattering order in this case is smoother than for forward scattering (Figs 3, 4). This is explained by random propagation directions of photons during multiple scattering, because scattering occurs at a random step due to a low probability of backward scattering. Note also that backward scattering does not exhibit such a nonuniform angular distribution as in the case of forward scattering, which is again explained by random propagation directions of backscattered photons.

Because the model parameters μ_s and g that we use cannot be measured directly, they are known with a certain accuracy. In this connection, it is important to know how the variation in these parameters can affect the simulation results. We analysed the dependence of the simulation results on these parameters by varying their values for both wavelengths. The results of these calculations are presented in Figs 5–8. One can see that the variation of μ_s affects the scattering intensity stronger than the variation of g. Thus, when μ_s was changed by 10 %, the intensity of scattering (at angles 50 and 150°) was changed by a factor of two, whereas a change in g by 1 % in the region of values close to unity resulted in the change of the scattering intensity by an order of magnitude. This occurs because in the first case the parameter of the medium itself was changed, while in the second case the parameter of each erythrocyte was changed, and the effect of the parameter g proves to be stronger due to the dominant role of multiple scattering. Physically, an increase in g corresponds to an increase in the average size of a scattering particle, while an increase in μ_s corresponds to an increase in the concen-

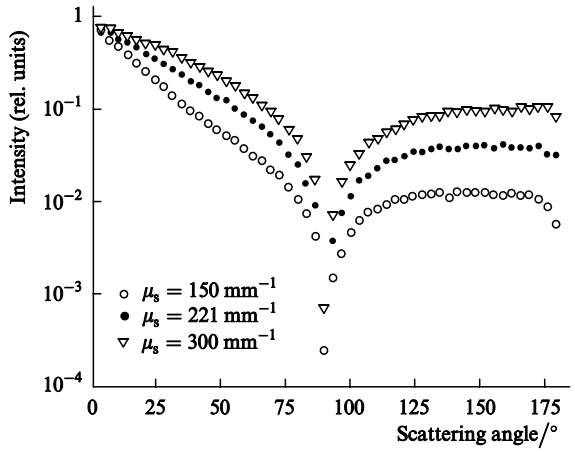

Figure 5. Dependences of the scattering indicatrix on the model parameter μ_s for $\lambda = 0.514$ μm, $\mu_a = 22.7$ mm^{-1}, $g = 0.972$, $d = 0.1$ mm. The calculation was performed for 10^6 photons.

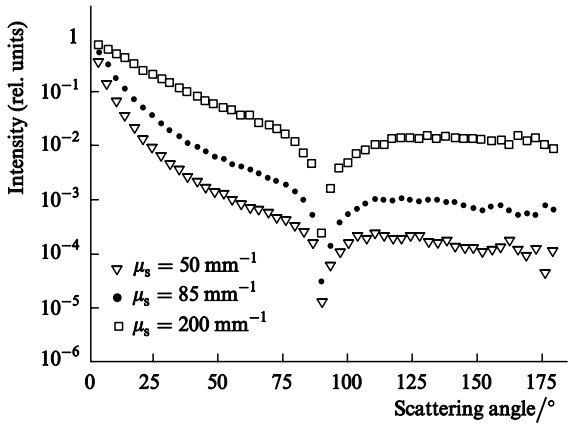

Figure 6. Dependences of the scattering indicatrix on the model parameter μ_s for $\lambda = 0.633$ μm, $\mu_a = 0.6$ mm^{-1}, $g = 0.980$, $d = 0.1$ mm. The calculation was performed for 10^6 photons.

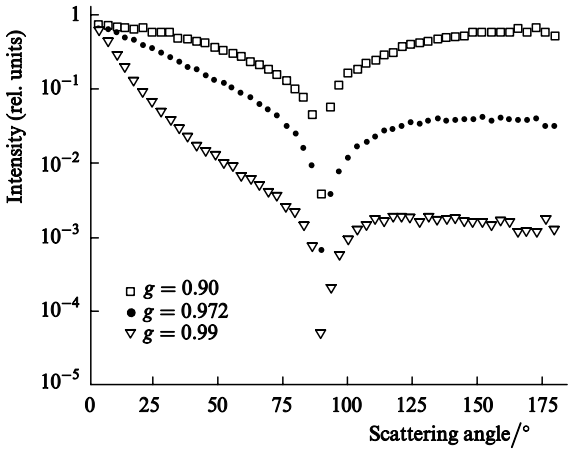

Figure 7. Dependences of the scattering indicatrix on the model parameter g for $\lambda = 0.514$ μm, $\mu_s = 221$ mm^{-1}, $\mu_a = 22.7$ mm^{-1}, $d = 0.1$ mm. The calculation was performed for 10^6 photons.

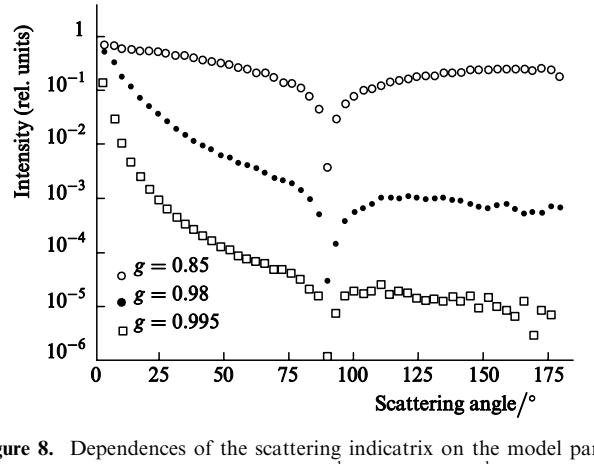

Figure 8. Dependences of the scattering indicatrix on the model parameter g for $\lambda = 0.633$ μm, $\mu_s = 85$ mm^{-1}, $\mu_a = 0.6$ mm^{-1}, $d = 0.1$ mm. The calculation was performed for 10^6 photons.

tration of scattering particles.

Because multiple scattering dominates in the process under study, it is important to know whether or not the diffuse approximation is applicable in this case. It was shown in paper [16] that this approximation adequately describes high-order scattering (for $n > l_{tr}/\langle L\rangle$, where l_{tr} is the transport length); however, to make certain conclusions, numerical estimates are required.

The criterion for applicability of the diffuse approximation has the form

$$\mu_a \ll \mu_s(1-g),$$

which means that this approximation cannot be used for $\lambda = 0.514$ μm, but can be used, with some restrictions, for $\lambda = 0.633$ μm.

4. Conclusions

We have shown that forward scattering of light by a layer of the erythrocyte suspension is mainly determined by snake photons, whose direction of propagation in the medium changes weakly. The intensity of backward scattering is characterised by more uniform distributions over angles and scattering orders. We have found that for parameters corresponding to the experimental conditions, the low-order scattering makes a small contribution to the total detected signal. We have shown that the diffuse approximation can be applied for simulating the propagation of light in the medium under study with substantial restrictions. We have analysed the stability of our results to variations in the model parameters μ_s and g, and found that, for parameters close to the real parameters of blood, the influence of g is much greater than of μ_s.

Acknowledgements. The authors thank V.V. Tuchin, V.V. Lopatin, and O.E. Fedorova for useful discussions. This work was supported by the Russian Foundation for Basic Research (Grant No. 00-1597-843 for the support of Leading Scientific Schools) and the Moscow State University Interdisciplinary Scientific Project 'Optics of Blood'.

References

1. Priezzhev A.V., Tuchin V.V., Shuochkin L.P. *Lazernya diagnostika v biologii i meditsine* (Laser Diagnostics in Biology and Medicine) (Moscow: Nauka, 1989).
2. Tuchin V.V. *Lazery i volokonnaya optika v biomeditsinskikh issledovaniyakh* (Lasers and Fibre Optics in Biomedical Studies) (Saratov: Izd. Saratov University, 1998).
3. Bohren C.F., Huffman D.R. *Absorption and Scattering of Light by Small Particles* (New York: Wiley, 1983; Moscow: Mir, 1986).
4. van de Hulst H.C. *Light Scattering by Small Particles* (New York: Wiley, 1957; Moscow: Inostrannaya Literatura, 1961).
5. Shepelevitch N.A., Lopatin V.N., Maltsev V.P., Lopatin V.V. *J. Opt. A: Pure Appl. Opt.*, **1**, 448 (1999).
6. Borovoi A.G., Naats E.I., Oppel U.G. *J. Biomed. Opt.*, **3**, 364 (1998).
7. Kandidov V.P. *Usp. Fiz. Nauk*, **166**, 1309 (1966).
8. Levtov V.A., Regirer S.A., Shadrina I.Kh. *Reologiya krovi* (Blood Reology) (Moscow: Medicine, 1982).
9. Johnson C.C., Guy A.V. *Proc. IEEE*, **6**, 692 (1972).
10. McRae R.A., McClure J.A., Latimer P. *J. Opt. Soc. Am.*, **12**, 1366 (1961).
11. Hammer M., Yaroslavsky A.N., Schweitzer D. *Physics in Medicine and Biology*, **46**, 65 (2001).
12. Rogan A., Friebel M., Dorschel K., Hahn A., Muller G. *J. Biomed. Opt.*, **4**, 36 (1999).
13. Sobol' I.M. *Chislennye metody Monte Karlo* (Numerical Monte Carlo Methods) (Moscow: Nauka, 1973).
14. Lopatin V.V., Priezzhev A.V., Fedoseev V.V. *Biomed. Radioelektron.*, **7**, 29 (2000).
15. Yaroslavsky A.N., Yaroslavsky I.V., Goldbach T., Schwarzmaier H.J. *J. Biomed. Opt.*, **4**, 47 (1999).
16. Skipetrov S.E., Chesnokov S.S. *Kvantovaya Elektron.*, **25**, 753 (1998) [*Quantum Electron.*, **28**, 733 (1998)].